

Fundamental and harmonic susceptibilities of $\text{YBa}_2\text{Cu}_3\text{O}_{7-\delta}$

T. Ishida

Department of Physics, Ibaraki University, Mito 310, Japan

R. B. Goldfarb

Electromagnetic Technology Division, National Institute of Standards and Technology, Boulder, Colorado 80303

(Received 15 November 1989)

We have examined the complex harmonic magnetic susceptibilities $\chi_n = \chi'_n - i\chi''_n$ ($n = 1, 2, 3, \dots, 10$) of the sintered high-critical-temperature (high- T_c) superconductor $\text{YBa}_2\text{Cu}_3\text{O}_{7-\delta}$. The experimental variables for the measurements of χ_n were the sample temperature T ($10 \leq T \leq 110$ K), the ac magnetic field amplitude H_{ac} ($1.4 \mu\text{T} \leq \mu_0 H_{ac} \leq 8.5$ mT), frequency f ($7.3 \leq f \leq 1460$ Hz), and the magnitude of a superimposed dc field H_{dc} ($|\mu_0 H_{dc}| \leq 8.5$ mT). As functions of temperature, χ'_1 and χ''_1 depend on both H_{ac} and H_{dc} . In particular, the χ'_1 transition curve can shift to *higher* temperatures with increasing H_{dc} . Odd-harmonic susceptibilities were measured as functions of temperature below T_c for zero H_{dc} ; both even and odd harmonics were observed for nonzero H_{dc} . At fixed temperature, the odd-harmonic susceptibilities are even functions of H_{dc} , while the even-harmonic susceptibilities are odd functions of H_{dc} . We compared the experimental intergrain coupling characteristics of χ'_n and χ''_n with theoretical susceptibility curves based on magnetization equations derived by Ji *et al.* from a simplified Kim model for critical current density. The theoretical curves are in good agreement with the temperature- and field-dependent features of χ'_n and χ''_n , and, therefore, the intergrain coupling component of a sintered high- T_c superconductor behaves as a type-II superconductor.

I. INTRODUCTION

A measurement of the superconducting transition by means of complex ac susceptibility $\chi = \chi' - i\chi''$ typically shows, just below the critical temperature T_c , a sharp decrease in χ' , a consequence of diamagnetic shielding, and a peak in χ'' , representing losses. This magnetic response was studied by Maxwell and Strongin,¹ Ishida and Mazaki,² Khoder,³ and Hein⁴ for conventional bulk superconductors.

Complex susceptibility is useful for characterizing high-critical-temperature (high- T_c) superconductors in conjunction with, or as an alternative to, resistivity, dc susceptibility, and specific heat. A sintered high- T_c superconductor, such as $\text{YBa}_2\text{Cu}_3\text{O}_{7-\delta}$ (Y-Ba-Cu-O), can be modeled as a system in which the superconducting grains are weakly coupled. In such materials, χ has both intrinsic and coupling components. The coupling component is very sensitive to both temperature T and the amplitude of the ac measuring field H_{ac} . Several experiments on the H_{ac} dependence of χ versus T have been reported.⁵⁻¹⁰

For an ac magnetic excitation field, $H(t) = H_{ac} \sin(\omega t)$, at the fundamental frequency ω ($\equiv 2\pi f_1$), the harmonic susceptibility may be represented as $\chi_n = \chi'_n - i\chi''_n$, where $n=1$ denotes the fundamental susceptibility. Bean's critical-state model for the magnetization of type-II superconductors, in which the critical current density J_c was assumed to be independent of the local magnetic field, predicted the existence of odd harmonics of susceptibility.¹¹

Experimentally, Ishida and Mazaki^{12,13} used the fundamental and higher-harmonic susceptibilities to study a multiconnected low-temperature superconductor, which they modeled as a network of microbridge-type weak links. The model qualitatively described the temperature and H_{ac} dependences of χ_1 for a weakly connected superconductor. It predicted the emergence of odd-harmonic susceptibilities below T_c and the proportionality of the magnitude of the third-harmonic susceptibility $|\chi_3|$ to χ''_1 , in good agreement with experiment. Harmonic susceptibility was also used to characterize a synthetic one-dimensional superconductor.¹⁴ The Ishida-Mazaki conclusions are in good agreement with experimental data and some interpretations for high- T_c superconductors.

Shaulov and Dorman¹⁵ compared χ'_1 and $|\chi_3|$ as functions of temperature and dc bias field for sintered Y-Ba-Cu-O. They detected a field-dependent transition temperature above which $|\chi_3|$ was zero but χ''_1 was not. They attributed this to a state of dissipative flux motion without pinning. Lam, Jeffries, and co-workers¹⁶⁻¹⁸ reported the nonlinear behavior of Y-Ba-Cu-O in a radio-frequency magnetic field. They modeled the system as a suitably averaged collection of flux-quantized supercurrent loops containing Josephson junctions and proposed a dynamic model for explaining the harmonic generation. A similar approach, with the addition of a field-dependent loop current, was presented by Xia and Stroud.¹⁹

Harmonic susceptibilities of high- T_c superconductors have been experimentally studied by others. Sato *et al.*²⁰ reported the third-harmonic susceptibility $\chi'_3 - i\chi''_3$ of sin-

tered Y-Ba-Cu-O and interpreted the harmonics as a superposition of the intrinsic and coupling contributions. Yamamoto *et al.*²¹ measured the third-harmonic susceptibility of single-crystal Y-Ba-Cu-O films in an ac magnetic field perpendicular to the film surface. Giovannella *et al.*,²² Lucchini *et al.*,²³ and Park *et al.*²⁴ interpreted measurements of harmonic susceptibility using a superconductor glass model. Lera *et al.*²⁵ and Navarro *et al.*²⁶ measured the harmonic susceptibilities of sintered Y-Ba-Cu-O and used them to reconstruct the magnetic hysteresis loop. Okamoto *et al.*²⁷ examined the third-harmonic content of the magnetic hysteresis loop as a function of dc bias field. Luzyanin *et al.*²⁸ measured the low-field dependence of the magnitude of the harmonic magnetization. Xenikos and Lemberger²⁹ measured the harmonic magnetization of single-crystal Y-Ba-Cu-O as a function of temperature just below T_c . They interpreted the results in terms of field- and temperature-dependent magnetoresistance.

Unlike the Bean model, the critical-state model by Kim *et al.*^{30,31} assumes a critical current density J_c that decreases with increasing local field H_i : $J_c = k / (H_0 + |H_i|)$, where k and H_0 are constants. Chen *et al.*³² computed the fundamental susceptibility based on Kim model equations for magnetization presented by Chen and Goldfarb.³³ Müller³⁴ calculated the temperature and field dependences of the fundamental susceptibility, including the intergranular contribution, using the Kim model and compared them to experimental results of Goldfarb *et al.*⁵ The Kim model has been shown to accurately predict many of the electromagnetic properties of the coupling component in sintered materials.^{28,35}

Müller *et al.*³⁶ and Ji *et al.*³⁷ investigated the effect of a superimposed dc field on the generation of even harmonics, which are not predicted by the Bean model. Müller *et al.*^{34,36} compared $|\chi_n|$ obtained with a spectrum analyzer to theoretical results derived using the Kim model. Ji *et al.*³⁷ used a simplified Kim model, in which H_0 was taken to be zero,³⁸ and derived equations for the magnetic hysteresis loop around a dc bias field for a slab geometry. Using these equations, they numerically computed $|\chi_n|$ and compared experimental data obtained with a Fourier signal analyzer.

In this paper, we present a detailed investigation of the validity of the simplified Kim model by comparing experimental and theoretical complex harmonic susceptibility. We measured the dependences of both χ'_n and χ''_n ($n \leq 10$) on temperature, ac field, and dc field using a lock-in amplifier rather than a signal analyzer. The higher harmonics result from hysteresis and nonlinearity of magnetization. We obtained good agreement of experimental data with the theoretical behavior deduced from the equations for magnetization of Ji *et al.*

Equations and results are expressed in SI units. Volume susceptibility is dimensionless, with full diamagnetism corresponding to a susceptibility of -1 . Applied magnetic fields H are given numerically as $\mu_0 H$, the flux density in free space, in units of teslas, where $\mu_0 = 4\pi \times 10^{-7}$ H/m. The conversion factor to cgs electromagnetic units is 10^{-4} T/G, where G is dimensionally and numerically equivalent to Oe.

II. EXPERIMENTAL MEASUREMENTS

A. Sample preparation

The $\text{YBa}_2\text{Cu}_3\text{O}_{7-\delta}$ samples were prepared by a solid-state reaction from Y_2O_3 , BaCO_3 , and CuO powders. The stoichiometric mixture was ground and reacted in air at 800°C for 19 h, 850°C for 9 h, 880°C for 22 h, and 800°C for 2 h. It was then cooled to room temperature in the furnace. It was reground, pelletized, and subsequently sintered in air at 800°C for 1 h, 900°C for 120 h, and cooled in the furnace.

The pellets were thoroughly oxidized in flowing oxygen at standard atmospheric pressure by using a programmable temperature controller. The temperature was increased linearly from 25 to 800°C in 2 h, held at 800°C for 22 h, decreased at a constant rate from 800 to 300°C in 48 h, kept at 300°C for 48 h, and decreased linearly from 300 to 25°C in 24 h. After the oxygen treatment, δ in the chemical formula decreased by approximately 0.025 based on the change in sample mass. We examined a 74%-dense Y-Ba-Cu-O specimen (9.2-mm diameter, 5.3-mm length, 1.658-g mass) by x-ray diffraction. The specimen was single phase and the lattice parameters were $a = 3.823\,03 \pm 0.000\,33$ Å, $b = 3.884\,69 \pm 0.000\,35$ Å, and $c = 11.661\,51 \pm 0.000\,09$ Å. The c value corresponds to $\delta = 0.036$.³⁹ The electrical resistivity of the Y-Ba-Cu-O sample was zero below 89.8 K.

We used this Y-Ba-Cu-O pellet for the measurement of the harmonic susceptibility. The demagnetization factor of the pellet was approximately 0.28 for ac and dc fields both applied perpendicular to the pellet axis,⁴⁰ but, for consistency in computing the harmonic susceptibilities, we did not correct the susceptibility data for demagnetization factor.

B. Definition of harmonic susceptibility

The fundamental susceptibility χ_1 has clear physical meaning. The real part χ'_1 corresponds to the dispersive magnetic response and the imaginary part χ''_1 corresponds to energy dissipation. χ'_1 reflects supercurrent shielding for superconductors. The external magnetic field $H(t)$ is

$$H(t) = H_{ac} \text{Im}(e^{i\omega t}) = H_{ac} \sin(\omega t),$$

where $\text{Im}(\)$ denotes the imaginary part of the complex variable. We define the magnetization $M(t)$ as a function of t by

$$\begin{aligned} M(t) &= H_{ac} \sum_{n=1}^{\infty} \text{Im}(\chi_n e^{in\omega t}) \\ &= H_{ac} \sum_{n=1}^{\infty} [\chi'_n \sin(n\omega t) - \chi''_n \cos(n\omega t)], \end{aligned} \quad (1)$$

where $\chi_n = \chi'_n - i\chi''_n$ ($n = 1, 2, 3, \dots$). This form of the complex variable is consistent with the physical meaning of χ_1 . χ'_n and χ''_n can be calculated by

$$\chi'_n = \frac{1}{\pi H_{ac}} \int_0^{2\pi} M(t) \sin(n\omega t) d(\omega t), \quad (2a)$$

$$\chi_n'' = \frac{-1}{\pi H_{ac}} \int_0^{2\pi} M(t) \cos(n\omega t) d(\omega t). \quad (2b)$$

The same definition is used when a dc magnetic field is superimposed on the ac field. (See the Appendix for the experimental implications of an alternative definition for harmonic susceptibility.) The function $M(t)$ consists of the appropriate equations for magnetization as a function of field $M(H)$,³³ in which H is expressed as $H(t) = H_{ac} \sin(\omega t)$. For analytic evaluation, the integrals in Eqs. (2a) and (2b) are separated into intervals $\pi/2$ to $3\pi/2$ and $3\pi/2$ to $5\pi/2$, corresponding to decreasing and increasing $H(t)$.

C. Measurement of harmonic susceptibility

Experimentally, we observe a voltage, proportional to the time derivative of $M(t)$, induced in a pickup coil,

$$\frac{d[M(t)]}{dt} = H_{ac} \sum_{n=1}^{\infty} [n\omega \chi_n' \cos(n\omega t) + n\omega \chi_n'' \sin(n\omega t)]. \quad (3)$$

We used a two-phase lock-in amplifier to separate the $\cos(n\omega t)$ and $\sin(n\omega t)$ parts. Consistent with our adopted sign convention, the lock-in reference was $\sin(n\omega t)$ and the outputs had positive polarities.

We measured each χ_n as a function of increasing temperature using a two-position ac susceptometer.^{41,42} Two-position measurements eliminate spurious contributions to the fundamental susceptibility signal from any pickup coil imbalance. The susceptometer was calibrated numerically and with standards.⁴⁰ A high-permeability shield around the Dewar reduced the Earth's field to less than $0.5 \mu\text{T}$ in the measurement axis. The sample was cooled to $\sim 5 \text{ K}$ in zero field to minimize trapped flux in the superconducting sample. Instrument control and measurements were computerized. Susceptibility data were taken at temperature intervals of $< 0.1 \text{ K}$ as the temperature of the specimen increased at a rate $< 0.4 \text{ K/min}$ near T_c .

The current to the primary field coil, proportional to $\sin(\omega t)$, was generated by an ac constant-current amplifier driven by one channel of a two-channel synthesizer. Frequency accuracy was $5 \mu\text{Hz}$. Second- and third-harmonic voltage distortion, measured with a signal analyzer across the susceptometer field coil, was less than 0.03% of the fundamental voltage (-70 dBV). The second synthesizer channel provided a reference voltage, proportional to $\sin(n\omega t)$, to the two-phase lock-in amplifier.

Correct phase adjustment is important for accurate separation of the real and imaginary parts of fundamental and harmonic susceptibilities. The procedure for each measurement of χ_n was as follows. With *both* synthesizer channels at the intended harmonic frequency nf_1 and in phase, we adjusted the lock-in phase angle to null χ_1'' for a measuring field amplitude of $1.4 \mu\text{T}$ at $\sim 7 \text{ K}$. (For small fields, there is perfect diamagnetic shielding and zero losses up to $\sim 80 \text{ K}$.) The lock-in phase adjustment would be maintained for measurements at higher temper-

atures, higher ac fields, and with superimposed dc fields. We then set the excitation synthesizer channel to the fundamental frequency f_1 , while the lock-in reference channel remained at nf_1 . The relative phase between the two synthesizer channels was then adjusted to zero using Lissajous figures on an oscilloscope. With these adjustments, the two outputs of the lock-in amplifier were proportional to $n\omega H_{ac} \chi_n'$ and $n\omega H_{ac} \chi_n''$.

Some harmonic susceptibility measurements were made at constant H_{ac} and temperature (4 or 76 K) as a function of H_{dc} using the dc offset of the synthesizer. Lock-in phase adjustment was accomplished as described above. The sample was warmed to above 90 K and cooled in zero field before stepping H_{dc} from zero to either a positive or a negative maximum. This precaution avoided initial trapped flux in the sample. Due to instrument limitations, the steps in applied dc field were not entirely monotonic and likely caused minor magnetization hysteresis loops to be traced before the field stabilized at each higher value. The result, however, would be the same as with a smooth field sweep.

III. MODEL CALCULATIONS

A. Bean model

The harmonic susceptibilities $\chi_n' - i\chi_n''$ can be evaluated analytically or numerically from equations of magnetization $M(t)$ as a function of field $H(t)$. We approximate the superconductor sample disk as an infinite slab for purposes of applying the critical-state model. The harmonic susceptibilities for an infinite slab, when H_{ac} is less than the full penetration field H_p , may be calculated analytically using the Bean equations for $M(H)$:

$$\chi_1' = H_{ac}/2H_p - 1, \quad (4a)$$

$$\chi_1'' = 2H_{ac}/3\pi H_p, \quad (4b)$$

$$\chi_n' = 0 \quad (n > 1), \quad (4c)$$

$$\chi_n'' = (-1)^{(n+1)/2} 2H_{ac} / [H_p \pi (n-2)n(n+2)] \quad (n \text{ odd}), \quad (4d)$$

$$\chi_n'' = 0 \quad (n \text{ even}). \quad (4e)$$

As noted by Ji *et al.*,³⁷ no even harmonics appear in the framework of the Bean model, neither when $H_{ac} > H_p$ nor when there is a superimposed dc field. The hysteresis loop corresponding to these harmonic susceptibilities is lenticular.^{11,25,26} Total loss per unit volume per field cycle is⁴³ $W = \pi\mu_0 H_{ac}^2 \chi_1''$. Losses are solely hysteretic in the critical-state model; Eq. (4b) represents hysteresis loss, as may be verified by comparing the equations for χ_1' and W .^{33,44}

B. Ishida-Mazaki model

Ishida and Mazaki^{12,13} gave expressions for the harmonic susceptibilities of a multiconnected Josephson network. They are equivalent to the formulation of Rollins and Silcox⁴⁵ for a bulk superconducting surface sheath. The equations are

$$\chi'_1 = (\frac{1}{2}\sin 2\alpha - \alpha)/\pi, \quad (5a)$$

$$\chi''_1 = (\sin^2\alpha)/\pi, \quad (5b)$$

$$\chi'_n = \frac{(-1)^{(n+1)/2}}{n\pi} \left[\frac{\sin(n+1)\alpha}{n+1} - \frac{\sin(n-1)\alpha}{n-1} \right] \quad (n \text{ odd}), \quad (5c)$$

$$\chi''_n = \frac{(-1)^{(n+1)/2}}{n\pi} \left[\frac{\cos(n+1)\alpha - 1}{n+1} - \frac{\cos(n-1)\alpha - 1}{n-1} \right] \quad (n \text{ odd}), \quad (5d)$$

$$\chi'_n = 0 \quad (n \text{ even}), \quad (5e)$$

$$\chi''_n = 0 \quad (n \text{ even}), \quad (5f)$$

where $\alpha \equiv 2\sin^{-1}(H_m/H_{ac})^{1/2}$ and H_m is the magnetic field which would induce a current equal to the critical current of the weak-link loop. The sign convention adopted here requires the factors $(-1)^{(n+1)/2}$ in the expressions for χ'_n and χ''_n . The Ishida-Mazaki model describes the essential features of the temperature and ac field dependences of χ_1 and $|\chi_3|$ for high- T_c and other multiconnected superconductors. Reconstruction of the magnetic hysteresis loop using the harmonic susceptibili-

ties gives a rhomboid. The model indicates nonzero χ'_n for $n > 1$ but, as in the case of the Bean model, it does not predict the even harmonics in a dc bias field.

C. Kim model

To account for the even harmonics and nonzero χ'_n , Ji *et al.*³⁷ derived equations for sample magnetization as a function of field

$$H(t) = H_{dc} + H_{ac}\sin(\omega t)$$

using a simplified Kim model, $J_c = k/|H_i|$, where k is a constant, and H_i is the local magnetic field. Although this form is discontinuous at $H_i = 0$, the integrations used to determine M are finite.³⁷ Susceptibility could then be obtained using Eqs. (2). For an infinite slab of thickness $2a$, the full penetration field H_p is $(2ka)^{1/2}$. The equations depend on the relative magnitudes of $2H_p^2$ and Δ^2 , where

$$\Delta^2 \equiv [H_a^2 \text{sgn}(H_a) - H_b^2 \text{sgn}(H_b)],$$

$$H_a \equiv H_{dc} + H_{ac}, \quad H_b \equiv H_{dc} - H_{ac},$$

$\text{sgn}(x) \equiv x/|x|$, for $x \neq 0$, and $\text{sgn}(x) \equiv 0$ for $x = 0$.

Because we used them in our analysis, the equations derived by Ji *et al.* are reproduced here for a sample cooled in zero field and never exposed to fields greater than $H(t)$.

For the case $\Delta^2 > 2H_p^2$, the magnetization $M(t)$ for $H(t)$ decreasing is

$$M(t) = [2/(3H_p^2)] \{ 2^{-1/2} |H(t)^2 \text{sgn}[H(t)] + H_a^2 \text{sgn}(H_a) |^{3/2} - |H(t)|^3 - |H_p^2 - H_a^2 \text{sgn}(H_a) |^{3/2} \} - H(t), \quad (6a)$$

when $H_a > H(t) > |H_a^2 \text{sgn}(H_a) - 2H_p^2|^{1/2} \text{sgn}[H_a^2 \text{sgn}(H_a) - 2H_p^2]$, and

$$M(t) = [2/(3H_p^2)] \{ |H(t)^2 \text{sgn}[H(t)] + H_p^2 |^{3/2} - |H(t)|^3 \} - H(t), \quad (6b)$$

when $|H_a^2 \text{sgn}(H_a) - 2H_p^2|^{1/2} \text{sgn}[H_a^2 \text{sgn}(H_a) - 2H_p^2] > H(t) > H_b$. The magnetization $M(t)$ for $H(t)$ increasing is

$$M(t) = -[2/(3H_p^2)] \{ 2^{-1/2} |H(t)^2 \text{sgn}[H(t)] + H_b^2 \text{sgn}(H_b) |^{3/2} - |H(t)|^3 - |H_p^2 + H_b^2 \text{sgn}(H_b) |^{3/2} \} - H(t), \quad (6c)$$

when $H_b < H(t) < |H_b^2 \text{sgn}(H_b) + 2H_p^2|^{1/2} \text{sgn}[H_b^2 \text{sgn}(H_b) + 2H_p^2]$, and

$$M(t) = -[2/(3H_p^2)] \{ |H(t)^2 \text{sgn}[H(t)] - H_p^2 |^{3/2} - |H(t)|^3 \} - H(t), \quad (6d)$$

when $|H_b^2 \text{sgn}(H_b) + 2H_p^2|^{1/2} \text{sgn}[H_b^2 \text{sgn}(H_b) + 2H_p^2] < H(t) < H_a$.

For the case $\Delta^2 < 2H_p^2$, the magnetization $M(t)$ for $H(t)$ decreasing from H_a to H_b is

$$M(t) = [2/(3H_p^2)] \{ 2^{-1/2} |H(t)^2 \text{sgn}[H(t)] + H_a^2 \text{sgn}(H_a) |^{3/2} - |H(t)|^3 - |\frac{1}{2}[H_a^2 \text{sgn}(H_a) + H_b^2 \text{sgn}(H_b)]|^{3/2} \} - H(t). \quad (7a)$$

The magnetization $M(t)$ for $H(t)$ increasing from H_b to H_a is

$$M(t) = -[2/(3H_p^2)] \{ 2^{-1/2} |H(t)^2 \text{sgn}[H(t)] + H_b^2 \text{sgn}(H_b) |^{3/2} - |H(t)|^3 - |\frac{1}{2}[H_a^2 \text{sgn}(H_a) + H_b^2 \text{sgn}(H_b)]|^{3/2} \} - H(t). \quad (7b)$$

The magnetic hysteresis loops obtained from these equations are minor loops, centered about any field, within the envelope of the symmetric astroid-shaped magnetization loop.^{33,38} A comparable but more protracted analysis using the *complete* Kim model was described by Müller.³⁴

We numerically obtained χ'_n and χ''_n using Eqs. (2) for various combinations of H_{ac} , H_{dc} , and H_p . The integrals

were evaluated using fast Fourier transforms (FFT) and double-precision variables. For the calculation, we sequentially generated 128 discrete values of $M(t)$ for one period of

$$H(t_i) = H_{dc} + H_{ac}\sin(\omega t_i)$$

using Eqs. (6) and (7).

D. Temperature dependence of susceptibility

The temperature dependence of susceptibility comes from that of J_c , k , or H_p . Ji *et al.*³⁷ assumed the two-fluid-model temperature dependence of J_c :

$$J_c \propto [1 - (T/T_c)^2][1 - (T/T_c)^4]^{1/2}.$$

Müller³⁴ used a different temperature dependence: $J_c \propto (1 - T/T_c)^2$ for the intergrain coupling component and $J_c \propto [1 - (T/T_c)^2]^2$ for the intrinsic intragrain component.

In fact, it is not necessary to assume a temperature dependence for J_c to describe the essential features of χ_n . In this work, we simply express the temperature dependence of χ'_n and χ''_n in terms of $H_p(T)$. H_p is zero at T_c . As T decreases from T_c , H_p increases monotonically. For $H_p \leq 0$, $\chi_n \equiv 0$. We find that H_p is a good proxy for temperature.

IV. RESULTS AND DISCUSSION

In this section we compare measured susceptibilities as functions of temperature to model calculations with the full penetration field H_p as the dependent variable. We also compare experimental and theoretical susceptibilities as functions of a superimposed dc field H_{dc} .

A. Fundamental susceptibility

Fundamental susceptibilities χ_1 were measured with the excitation field and the lock-in amplifier reference both at 73 Hz. We examine ac- and dc-field effects.

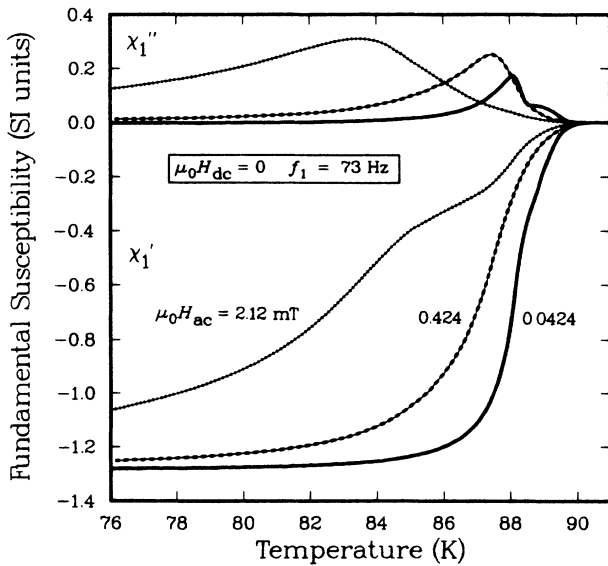


FIG. 1. Real and imaginary parts of fundamental susceptibility, χ'_1 and χ''_1 , of the Y-Ba-Cu-O pellet as a function of temperature for three different H_{ac} ($\mu_0 H_{ac} = 0.0424$, 0.424, and 2.12 mT), $H_{dc} = 0$, $f_1 = 73$ Hz. The data are not corrected for sample demagnetization factor.

1. Effect of ac field

In Fig. 1, we show the fundamental susceptibility (χ'_1 and χ''_1) at 73 Hz of the Y-Ba-Cu-O pellet as a function of temperature for three ac-field amplitudes ($\mu_0 H_{ac} = 0.0424$, 0.424, and 2.12 mT) in zero dc field. The data in this figure, as in all the figures, represent the external susceptibility, not corrected for demagnetization factor. Demagnetization correction would cause χ' to approach -1 at low temperature.

These experimental curves have intrinsic granular components and intergranular coupling components. χ''_1 shows two peaks corresponding to the intrinsic and coupling components. As H_{ac} increases, the height and breadth of the two peaks increase as they move to lower temperature. For $\mu_0 H_{ac} = 0.424$ mT, the intrinsic and coupling components happen to form a composite curve. A further increase of H_{ac} causes a two-step structure in χ'_1 and a shoulder in χ''_1 . These features are well known.⁵⁻¹⁰

For comparison of theory and experiment, we concentrate on the intergranular *coupling* component because it dominates the curves in Fig. 1. (The comparison could be made for the intrinsic grains by using much larger fields H_{ac} , H_{dc} , and H_p .) Figure 2 shows model calculations of χ'_1 and χ''_1 as functions of H_p for three ac fields ($\mu_0 H_{ac} = 0.0424$, 0.424, and 2.12 mT) in zero dc field. The curves are consistent with the calculations by Chen *et al.* in the slab limit.³² Use of the complete, rather than simplified, Kim model would reduce the height of the χ''_1 peaks in Fig. 2 (see Müller³⁴). As discussed above, H_p is a monotonically decreasing function of increasing temperature.

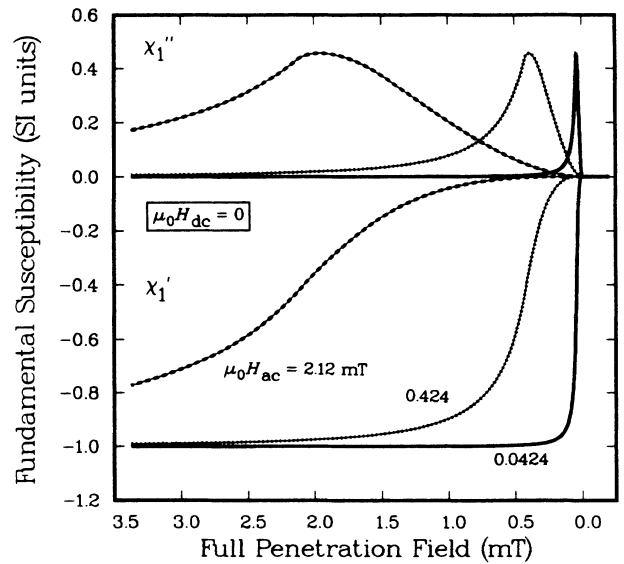


FIG. 2. Model calculations of the real and imaginary parts of fundamental susceptibility, χ'_1 and χ''_1 , for a superconductor as a function of full penetration field H_p for three different H_{ac} ($\mu_0 H_{ac} = 0.0424$, 0.424, and 2.12 mT), $H_{dc} = 0$, $f_1 =$ arbitrary. H_p is a monotonically decreasing function of increasing temperature.

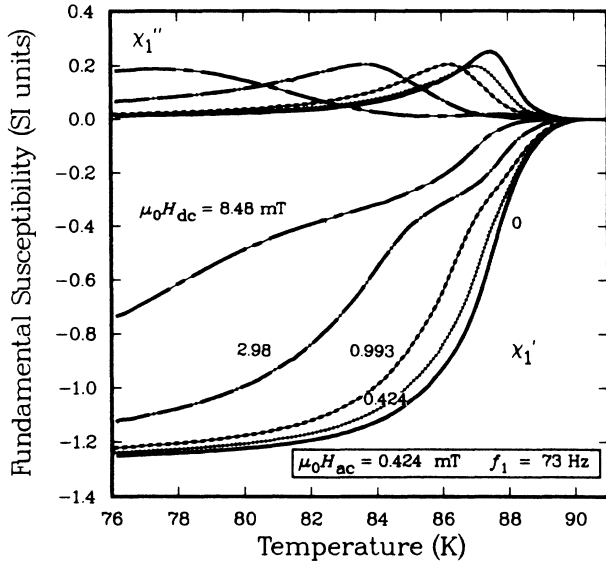


FIG. 3. Fundamental susceptibilities χ_1' and χ_1'' of the Y-Ba-Cu-O pellet as a function of temperature for five different H_{dc} ($\mu_0 H_{dc} = 0, 0.424, 0.993, 2.98,$ and 8.48 mT), $\mu_0 H_{ac} = 0.424$ mT, $f_1 = 73$ Hz. Note the decrease in χ_1' coupling peak height for applied dc fields.

perature. The figure is scaled to demonstrate similarity with the coupling components in Fig. 1. The model does not explain the change in height of the χ_1'' peaks with H_{ac} seen experimentally.

2. Effect of dc field

In Fig. 3, we show χ_1' and χ_1'' of the Y-Ba-Cu-O pellet as functions of temperature for five dc bias fields

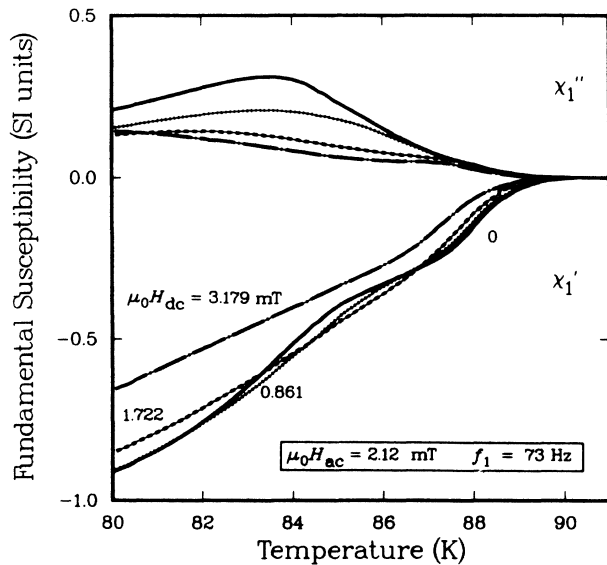


FIG. 5. Fundamental susceptibilities χ_1' and χ_1'' of the Y-Ba-Cu-O pellet as a function of temperature for four different H_{dc} ($\mu_0 H_{dc} = 0, 0.861, 1.722,$ and 3.179 mT), $\mu_0 H_{ac} = 2.12$ mT, $f_1 = 73$ Hz. The relatively large ac field makes apparent the shift in the χ_1' coupling transition to higher temperature with increasing dc field.

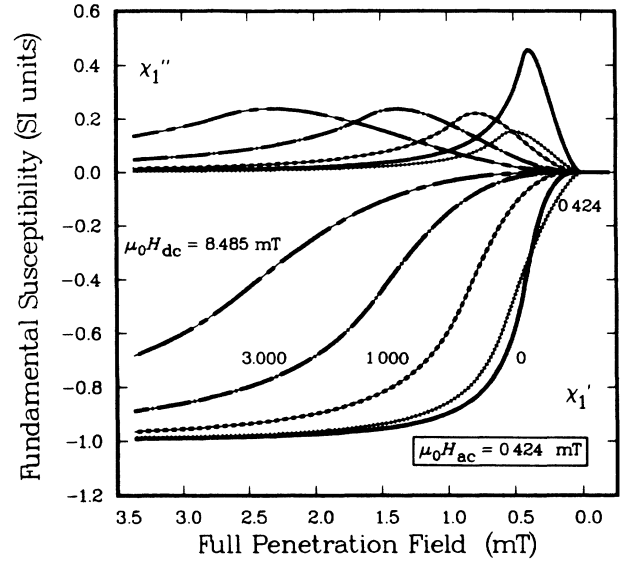


FIG. 4. Model calculations of the fundamental susceptibilities χ_1' and χ_1'' as a function of H_p for five different H_{dc} ($\mu_0 H_{dc} = 0, 0.424, 1.00, 3.00,$ and 8.485 mT), $\mu_0 H_{ac} = 0.424$ mT, $f_1 =$ arbitrary. For an applied dc field, the χ_1'' peak decreases in height and the χ_1'' transition shifts to lower temperature.

($\mu_0 H_{dc} = 0, 0.424, 0.993, 2.98,$ and 8.48 mT), for $\mu_0 H_{ac} = 0.424$ mT and $f_1 = 73$ Hz. The χ_1' curves decrease as a function of decreasing temperature in a two-step manner at higher H_{dc} . This is similar to the effect of higher ac fields in Fig. 1. The peak height of χ_1'' decreases appreciably for a dc field of 0.424 mT and above. This is not the case for the ac-field dependence in Fig. 1.

In Fig. 4, we show calculated curves of χ_1' and χ_1'' as

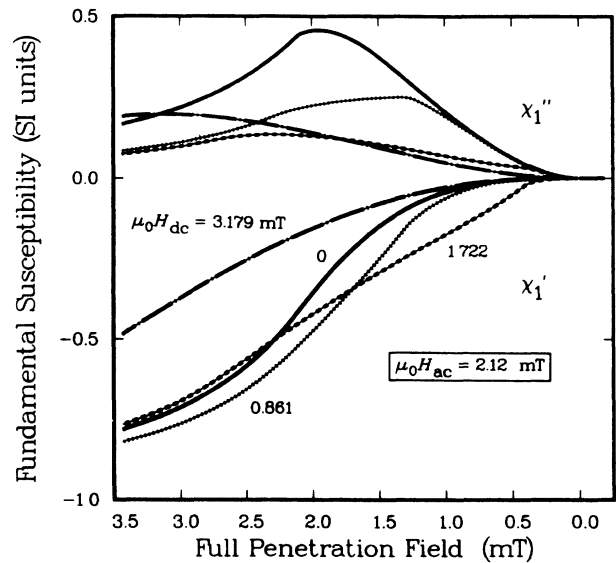


FIG. 6. Model calculations of the fundamental susceptibilities χ_1' and χ_1'' as a function of H_p for four different H_{dc} ($\mu_0 H_{dc} = 0, 0.861, 1.722,$ and 3.179 mT), $\mu_0 H_{ac} = 2.12$ mT, $f_1 =$ arbitrary.

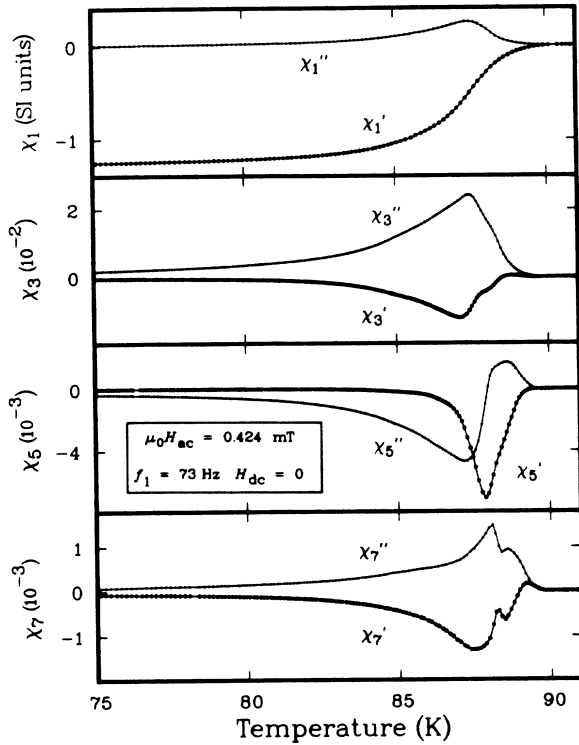


FIG. 7. Odd-harmonic susceptibilities χ'_n and χ''_n ($n=1,3,5,7$) of the Y-Ba-Cu-O pellet as a function of temperature. The measurement parameters were $\mu_0 H_{ac}=0.424$ mT, $H_{dc}=0$, and $f_1=73$ Hz.

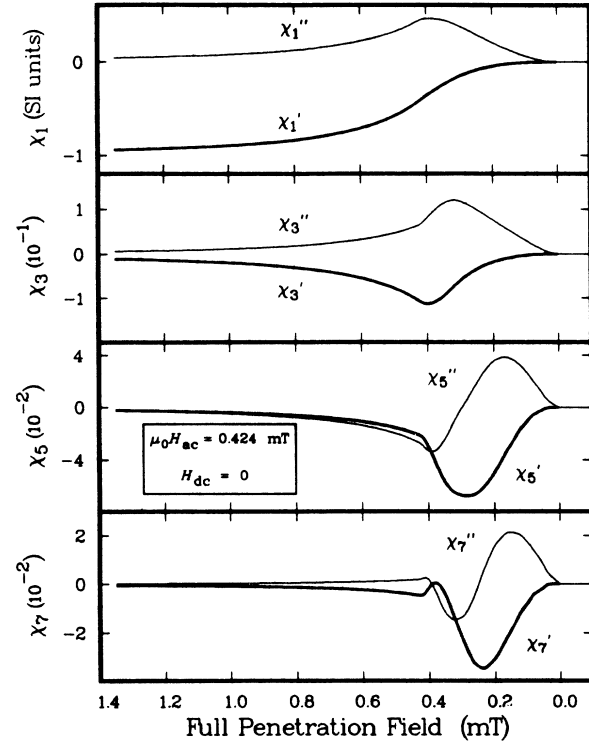


FIG. 8. Model calculations of the odd-harmonic susceptibilities χ'_n and χ''_n ($n=1,3,5,7$) of a superconductor as a function of H_p ; $\mu_0 H_{ac}=0.424$ mT, $H_{dc}=0$, f_1 = arbitrary.

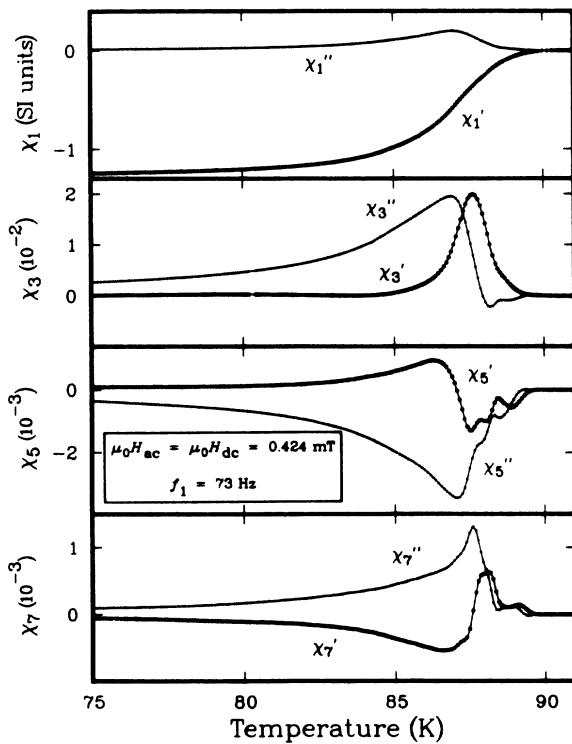


FIG. 9. Odd-harmonic susceptibilities χ'_n and χ''_n ($n=1,3,5,7$) of the Y-Ba-Cu-O pellet as a function of temperature for a superimposed dc magnetic field. The measurement parameters were $\mu_0 H_{ac}=0.424$ mT, $\mu_0 H_{dc}=0.424$ mT, and $f_1=73$ Hz.

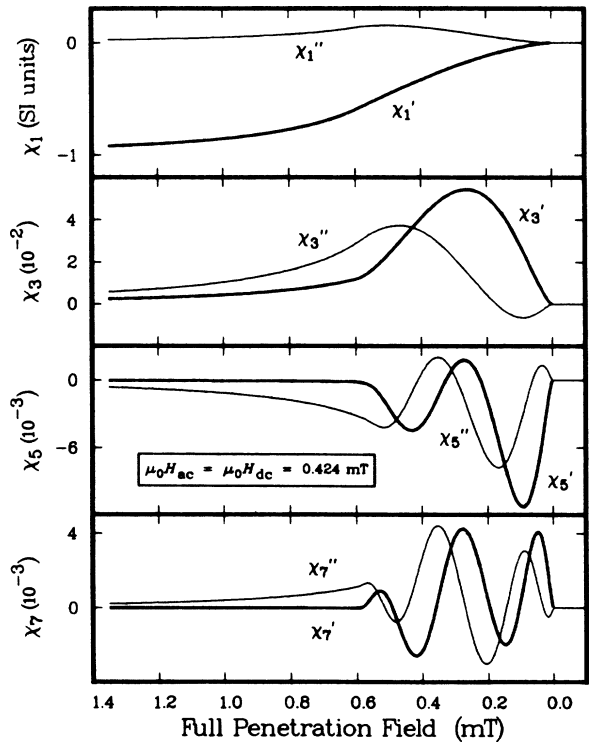


FIG. 10. Model calculations of the odd-harmonic susceptibilities χ'_n and χ''_n ($n=1,3,5,7$) of a superconductor as a function of H_p ; $\mu_0 H_{ac}=0.424$ mT, $\mu_0 H_{dc}=0.424$ mT, f_1 = arbitrary.

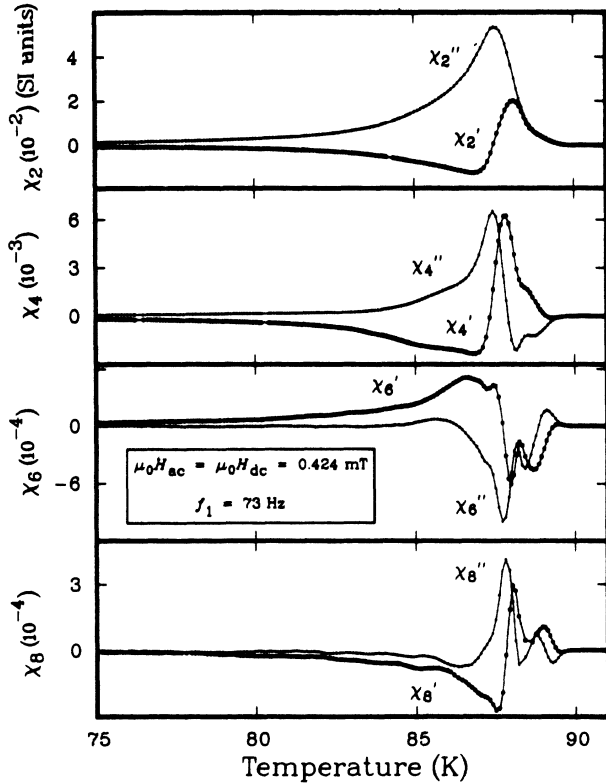


FIG. 11. Even-harmonic susceptibilities χ'_n and χ''_n ($n=2,4,6,8$) of the Y-Ba-Cu-O pellet as a function of temperature for a superimposed dc magnetic field. The measurement parameters were $\mu_0 H_{ac}=0.424$ mT, $\mu_0 H_{dc}=0.424$ mT, and $f_1=73$ Hz.

functions of decreasing H_p for similar conditions as in Fig. 3. As the dc field is applied, the χ''_1 peak height decreases as in the experimental curves in Fig. 3 and as modeled by Müller.³⁴ However, the transition in theoretical χ'_1 initially shifts to higher temperature. We explore this phenomenon further in Figs. 5 and 6. In Fig. 5 we show experimental χ'_1 and χ''_1 for a relatively large ac field $\mu_0 H_{ac}$ of 2.12 mT at 73 Hz, with dc fields $\mu_0 H_{dc}$ ranging from 0 to 3.18 mT. We note a positive shift in the coupling transition in χ'_1 with increasing H_{dc} , more emphasized than in Fig. 4. In Fig. 6, theoretical curves as functions of decreasing H_p for the corresponding parameters show the same effect. These curves, of course, refer to a single-component superconductor. Gömöry and Lobotka⁴⁶ and Giovannella *et al.*²² reported the dc-field dependence of χ'_1 and χ''_1 as functions of temperature. They did not examine the reduction of χ''_1 peak height or the positive shift in χ'_1 as H_{dc} increases.

B. Higher-harmonic susceptibility

Unlike the fundamental susceptibilities, the higher-harmonic real parts χ'_n and imaginary parts χ''_n are not constrained to negative and positive values, respectively. The superposition of a dc field permits the even harmonics.

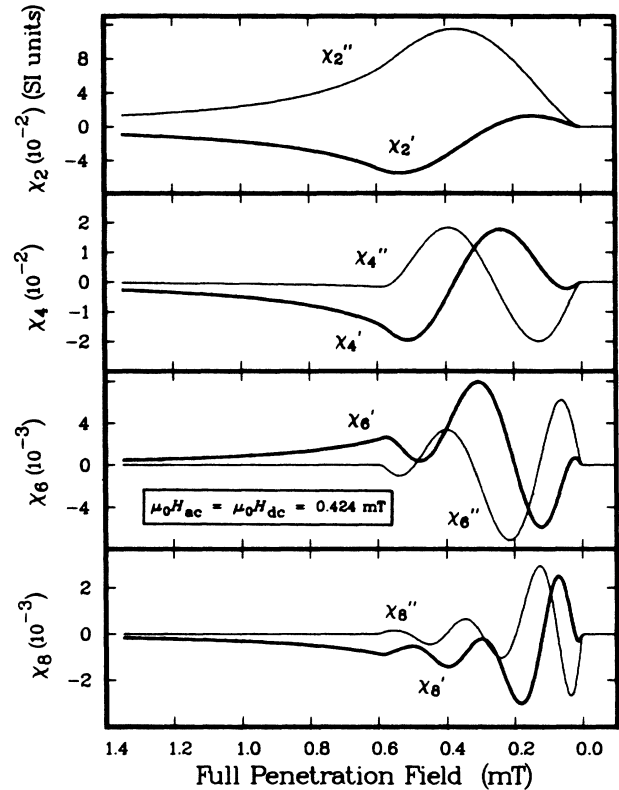


FIG. 12. Model calculations of the even-harmonic susceptibilities χ'_n and χ''_n ($n=2,4,6,8$) of a superconductor as a function of H_p ; $\mu_0 H_{ac}=0.424$ mT, $\mu_0 H_{dc}=0.424$ mT, f_1 =arbitrary.

1. Odd harmonics in ac field

In Fig. 7, we show experimental odd-harmonic susceptibilities χ'_n and χ''_n ($n=1,3,5,7$) of the Y-Ba-Cu-O pellet as functions of temperature for an ac field $\mu_0 H_{ac}=0.424$ mT at $f_1=73$ Hz. The ninth harmonic was measured but is not shown. There was no applied dc field. There is good qualitative correspondence with theoretical curves shown in Fig. 8. Quantitative agreement could be improved by using the complete Kim model, as discussed above. As noted by Lucchini *et al.*,²³ the fine structure in the higher-order harmonics is due to intrinsic granular and intergranular coupling critical transitions.

2. Even harmonics in ac field

Even harmonics were detected for zero H_{dc} at the 10^{-5} level in susceptibility. In principle, the appearance of these small harmonic susceptibilities could be attributed to even-harmonic content of H_{ac} , a slight dc offset in the constant-current amplifier, or residual ambient dc fields. Even harmonics are not expected for symmetric hysteresis loops centered at zero field.

3. Odd and even harmonics in superimposed ac and dc fields

In Fig. 9, we show the odd-harmonic susceptibilities χ'_n and χ''_n ($n=1,3,5,7$) of the Y-Ba-Cu-O pellet as func-

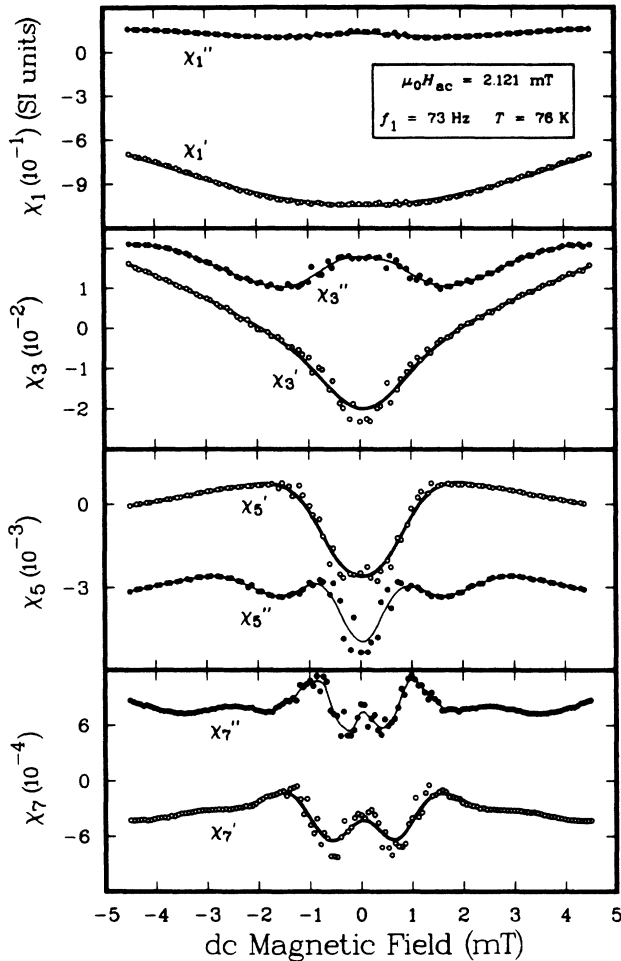


FIG. 13. Odd-harmonic susceptibilities χ'_n and χ''_n ($n=1,3,5,7$) as functions of H_{dc} ; $T=76$ K, $\mu_0 H_{ac}=2.121$ mT, $f_1=73$ Hz. The curves were obtained by cubic-spline smoothing.

tions of temperature for an ac field $\mu_0 H_{ac}=0.424$ mT at $f_1=73$ Hz. The ninth harmonic is not shown. There was a superimposed dc field $\mu_0 H_{dc}=0.424$ mT. The theoretical curves are shown in Fig. 10. They are quite different from the theoretical curves for $H_{dc}=0$ in Fig. 8.

In Fig. 11, we show the even-harmonic susceptibilities χ'_n and χ''_n ($n=2,4,6,8$) of the Y-Ba-Cu-O pellet as functions of temperature for an ac field $\mu_0 H_{ac}=0.424$ mT at $f_1=73$ Hz. The tenth harmonic is not shown. There was a superimposed dc field $\mu_0 H_{dc}=0.424$ mT. The theoretical curves are shown in Fig. 12.

The signs of the harmonics depend on the polarity of the superimposed dc field. We observed, for example, that the curves of second harmonic susceptibilities χ'_2 and χ''_2 as functions of T both shift phase by π (change their sign) for a negative dc bias field.

4. Field and frequency dependences of third-harmonic susceptibility

The third-harmonic susceptibilities χ'_3 and χ''_3 are the strongest and the most easily measured of the higher har-

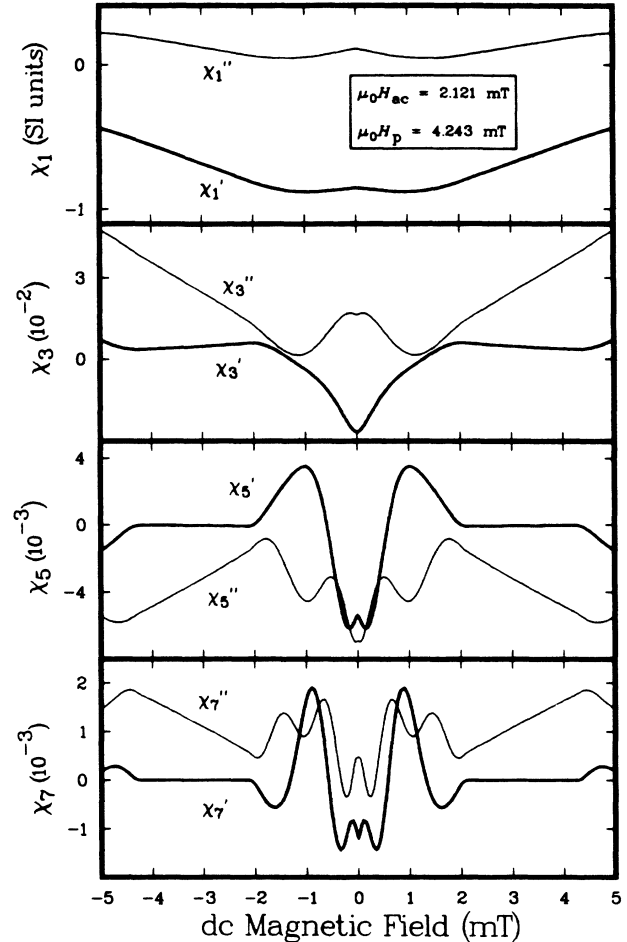


FIG. 14. Model calculations of odd-harmonic susceptibilities χ'_n and χ''_n ($n=1,3,5,7$) as functions of H_{dc} ; $\mu_0 H_p=4.243$ mT, $\mu_0 H_{ac}=2.121$ mT, f_1 =arbitrary.

monics. We measured the third-harmonic susceptibilities χ'_3 and χ''_3 of the Y-Ba-Cu-O pellet as functions of temperature for different ac fields H_{ac} . The shift of the coupling transition with increasing ac field is similar to the behavior of the fundamental (Fig. 1). The increase in magnitudes of χ'_3 and χ''_3 with increasing H_{ac} reflects the increase in nonlinearity, including hysteresis, in the magnetization as a function of field.

There were subtle frequency effects in the range $7.3 \leq f_1 \leq 1460$ Hz. These appeared as slight changes in the shapes of $\chi'_3(T)$ and $\chi''_3(T)$. In addition, there were small shifts in the temperature position of the coupling peak in $|\chi_3|$ of similar magnitude to frequency shifts seen in the χ''_1 coupling peak.⁴⁷ The Kim model, and other critical-state models, do not predict frequency-dependent susceptibilities.

C. Effect of dc field at constant temperature

We measured the dc-field dependence of harmonic susceptibility with the sample immersed in liquid nitrogen at 76 K. The odd harmonics were even functions of dc field

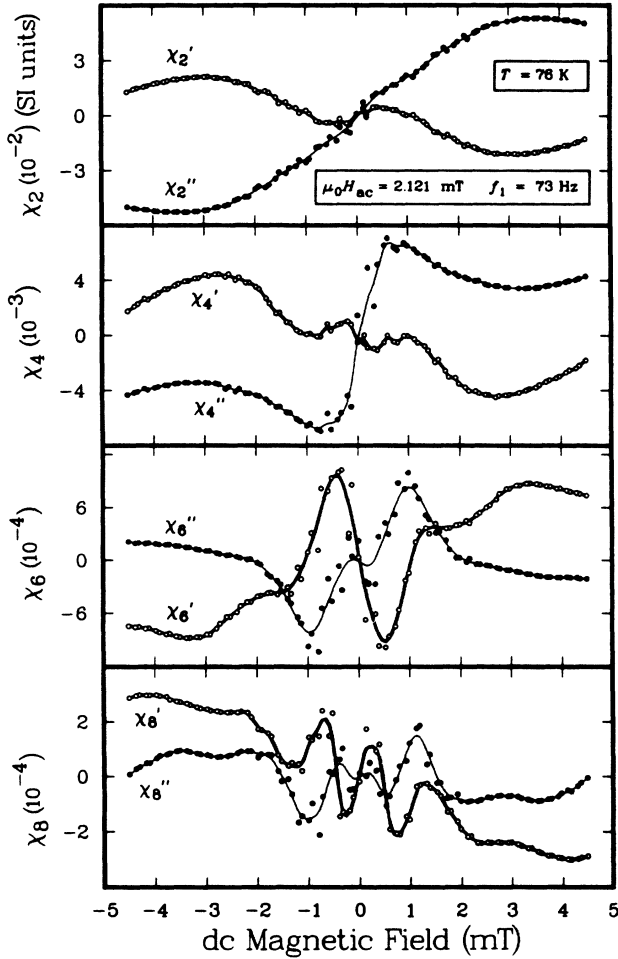


FIG. 15. Even-harmonic susceptibilities χ'_n and χ''_n ($n=2,4,6,8$) as functions of H_{dc} ; $T=76$ K, $\mu_0 H_{ac}=2.121$ mT, $f_1=73$ Hz. The curves were obtained by cubic-spline smoothing.

and the even harmonics were odd functions of dc field. This was also true in measurements at 4 K. By selecting the appropriate ac-field amplitude H_{ac} , and modeling with a full penetration field H_p twice as large, we are able to reproduce the key features of all the experimental curves.

Figure 13 shows the odd harmonics for $\mu_0 H_{ac}=2.121$ mT and $-4.5 < \mu_0 H_{dc} < 4.5$ mT. The theoretical curves in Fig. 14 are similar, but show more detail. Figures 15 and 16 show the experimental and theoretical even harmonics. Good quantitative agreement was obtained for $n < 5$.

V. CONCLUSION

We investigated the intergrain coupling characteristics of sintered Y-Ba-Cu-O by means of the harmonic susceptibilities χ'_n and χ''_n . Like the fundamental χ'_1 , the higher harmonics are manifestations of hysteresis and nonlinearity of the magnetization. (As pointed out by Shaulov and Dorman,¹⁵ χ'_1 could also result from hysteretic but *linear* behavior.) We compared the experimental results with

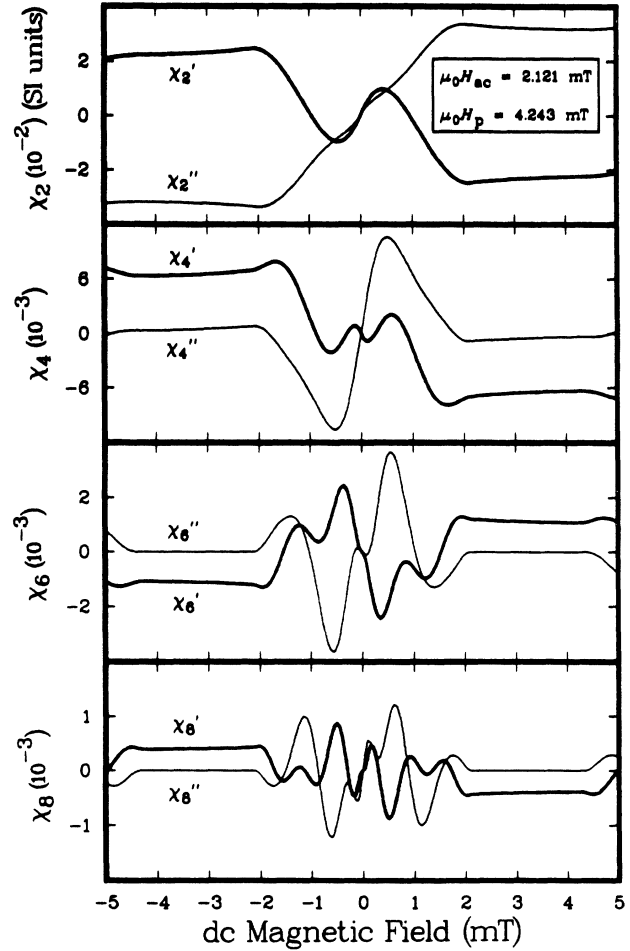


FIG. 16. Model calculations of even-harmonic susceptibilities χ'_n and χ''_n ($n=2,4,6,8$) as functions of H_{dc} ; $\mu_0 H_p=4.243$ mT, $\mu_0 H_{ac}=2.121$ mT, f_1 arbitrary.

theoretical susceptibility curves based on equations derived by Ji *et al.* from a simplified Kim model for critical-current density. The theoretical curves are in good agreement with the temperature- and field-dependent features of χ'_n and χ''_n . This is evidence that the intergrain coupling component has all the features of a type-II superconductor with reduced J_c , H_p , and T_c . Based on the results of experiments in which the coupling component is shown to disappear upon powdering,⁴⁸⁻⁵⁰ we surmise that coupling is achieved by the proximity effect or by microbridges. In principle, agreement with the model for intrinsic intragrain properties could be tested using a high-field ac susceptometer.

The simplified Kim model tends to exaggerate the magnetization near zero field,³³ magnifying χ'_1 and $|\chi_3|$. Numerical agreement between experiment and theory is improved if the complete Kim model is used, as was done by Müller *et al.* for χ'_1 and χ''_1 as functions of temperature³⁴ and for $|\chi_n|$ at a fixed temperature.³⁶ Alternative approaches, such as dynamic-loop¹⁶⁻¹⁹ and nonlinear-magnetoresistance²⁹ models have been used with some success to explain the harmonic power spectrum, $|\chi_n|$.

By comparing theoretical and experimental susceptibility curves and using a realistic model for the magnetization process, one could deduce $H_p(T)$ and $J_c(T)$. The experimental behavior of the higher harmonics, particularly the complex form $\chi'_n - i\chi''_n$, serves as an important test of the Kim critical-state model or other models.

ACKNOWLEDGMENTS

We benefited from expert computer programming by A. B. Kos and R. J. Loughran and helpful comments and suggestions by I. B. Goldberg. We thank L. Ji and co-authors, Harvard University, for a copy of their paper in advance of publication. T.I. expresses his thanks for the hospitality extended to him while he was a guest at the National Institute of Standards and Technology, Boulder, Colorado. Part of the work was supported by a grant-in-aid for scientific research from the Ministry of Education, Science, and Culture of Japan.

APPENDIX: ALTERNATIVE DEFINITION FOR HARMONIC SUSCEPTIBILITY

In this paper, we defined the applied magnetic field as

$$H(t) = H_{ac} \text{Im}(e^{i\omega t}) = H_{ac} \sin(\omega t),$$

where $\text{Im}(\)$ denotes the imaginary part of the complex variable. An alternative definition of the harmonic susceptibility is for an applied field

$$H(t) = H_{ac} \text{Re}(e^{i\omega t}) = H_{ac} \cos(\omega t),$$

where $\text{Re}(\)$ denotes the real part. In this case, the magnetization $M(t)$ is

$$\begin{aligned} M(t) &= H_{ac} \sum_{n=1}^{\infty} \text{Re}(\kappa_n e^{in\omega t}) \\ &= H_{ac} \sum_{n=1}^{\infty} [\kappa'_n \cos(n\omega t) + \kappa''_n \sin(n\omega t)]. \end{aligned} \quad (\text{A1})$$

The harmonic susceptibilities $\kappa_n = \kappa'_n - i\kappa''_n$ ($n = 1, 2, 3, \dots$) can be evaluated by

$$\begin{aligned} \kappa'_n &= \frac{1}{\pi H_{ac}} \int_0^{2\pi} M(t) \cos(n\omega t) d(\omega t), \\ \kappa''_n &= \frac{1}{\pi H_{ac}} \int_0^{2\pi} M(t) \sin(n\omega t) d(\omega t). \end{aligned} \quad (\text{A2})$$

The physical meanings of κ'_1 and κ''_1 are preserved by this definition.

We can relate χ_n to κ_n as

$$\begin{aligned} \chi'_{4m-3} &= \kappa'_{4m-3}, & \chi''_{4m-3} &= \kappa''_{4m-3}, \\ \chi'_{4m-2} &= -\kappa''_{4m-2}, & \chi''_{4m-2} &= \kappa'_{4m-2}, \\ \chi'_{4m-1} &= -\kappa'_{4m-1}, & \chi''_{4m-1} &= -\kappa''_{4m-1}, \\ \chi'_{4m} &= \kappa''_{4m}, & \chi''_{4m} &= -\kappa'_{4m}, \end{aligned} \quad (\text{A3})$$

where $m = 1, 2, 3, \dots$. In complex notation, $\chi_n = (-1)^{(3n+1)/2} \kappa_n$, $n = 1, 2, 3, \dots$. Note that the real and imaginary parts are *interchanged* for even harmonics, but $|\chi_n|$ is always equal to $|\kappa_n|$ for all n . These relations should be kept in mind for interlaboratory comparisons of the harmonic susceptibilities as well as for theoretical calculations.

¹E. Maxwell and M. Strongin, Phys. Rev. Lett. **10**, 212 (1963).
²T. Ishida and H. Mazaki, Phys. Rev. B **20**, 131 (1979).
³A. F. Khoder, Phys. Lett. **94A**, 378 (1983).
⁴R. A. Hein, Phys. Rev. B **33**, 7539 (1986).
⁵R. B. Goldfarb, A. F. Clark, A. I. Braginski, and A. J. Panson, Cryogenics **27**, 475 (1987).
⁶H. Mazaki, M. Takano, R. Kanno, and Y. Takeda, Jpn. J. Appl. Phys. **26**, L780 (1987).
⁷T. Ishida and H. Mazaki, Jpn. J. Appl. Phys. **26**, L1296 (1987).
⁸J. García, C. Rillo, F. Lera, J. Bartolomé, R. Navarro, D. H. A. Blank, and J. Flokstra, J. Magn. Magn. Mater. **69**, L225 (1987).
⁹H. Küpfer, I. Apfelstedt, W. Schauer, R. Flükiger, R. Meier-Hirmer, and H. Wühl, Z. Phys. B **69**, 159 (1987).
¹⁰D.-X. Chen, J. Nogués, N. Karpe, and K. V. Rao, Kexue Tongbao **33**, 560 (1988).
¹¹C. P. Bean, Rev. Mod. Phys. **36**, 31 (1964).
¹²T. Ishida and H. Mazaki, J. Appl. Phys. **52**, 6798 (1981).
¹³T. Ishida and H. Mazaki, Phys. Lett. **87A**, 373 (1982).
¹⁴T. Ishida, K. Kanoda, H. Mazaki, and I. Nakada, Phys. Rev. B **29**, 1183 (1984).
¹⁵A. Shaulov and D. Dorman, Appl. Phys. Lett. **53**, 2680 (1988).
¹⁶Q. H. Lam and C. D. Jeffries, Phys. Rev. B **39**, 4772 (1989).
¹⁷C. D. Jeffries, Q. H. Lam, Y. Kim, C. M. Kim, A. Zettl, and M. P. Klein, Phys. Rev. B **39**, 526 (1989).

¹⁸C. D. Jeffries, Q. H. Lam, Y. Kim, L. C. Bourne, and A. Zettl, Phys. Rev. B **37**, 9840 (1989).
¹⁹T.-K. Xia and D. Stroud, Phys. Rev. B **39**, 4792 (1989).
²⁰M. Sato, T. Kamimura, and T. Iwata, Jpn. J. Appl. Phys. **28**, 330 (1989).
²¹K. Yamamoto, H. Mazaki, H. Yasuoka, K. Hirata, T. Terashima, K. Iijima, and Y. Bando, Jpn. J. Appl. Phys. **28**, L1568 (1989).
²²C. Giovannella, C. Lucchini, B. Lecuyer, and L. Fruchter, IEEE Trans. Magn. **MAG-25**, 3521 (1989).
²³C. Lucchini, C. Giovannella, R. Messi, B. Lecuyer, L. Fruchter, and M. Iannuzzi, Phys. Status Solidi B (to be published).
²⁴K. Park, J. J. Kim, and J. C. Park, Solid State Commun. **71**, 743 (1989).
²⁵F. Lera, R. Navarro, C. Rillo, J. Bartolomé, J. Blasco, J. García, and L. A. Angurel, Physica C **162-164**, 325 (1989).
²⁶R. Navarro, F. Lera, C. Rillo, and J. Bartolomé, Physica C (to be published).
²⁷K. Okamoto, Y. Makino, N. Watanabe, and K. V. Rao, J. Appl. Phys. (to be published).
²⁸I. D. Luzyanin, S. L. Ginzburg, V. P. Khavronin, and G. Yu. Logvinova, Phys. Lett. A **141**, 85 (1989).
²⁹D. G. Xenikos and T. R. Lemberger, Phys. Rev. B **41**, 869 (1990).

- ³⁰Y. B. Kim, C. F. Hempstead, and A. R. Strnad, *Phys. Rev. Lett.* **9**, 306 (1962).
- ³¹Y. B. Kim, C. F. Hempstead, and A. R. Strnad, *Phys. Rev.* **129**, 528 (1963).
- ³²D.-X. Chen, J. Nogués, and K. V. Rao, *Cryogenics* **29**, 800 (1989).
- ³³D.-X. Chen and R. B. Goldfarb, *J. Appl. Phys.* **66**, 2489 (1989).
- ³⁴K.-H. Müller, *Physica C* **159**, 717 (1989).
- ³⁵K.-H. Müller, J. C. MacFarlane, and R. Driver, *Physica C* **158**, 69 (1989).
- ³⁶K.-H. Müller, J. C. MacFarlane, and R. Driver, *Physica C* **158**, 366 (1989).
- ³⁷L. Ji, R. H. Sohn, G. C. Spalding, C. J. Lobb, and M. Tinkham, *Phys. Rev. B* **40**, 10936 (1989).
- ³⁸M. C. Ohmer and J. P. Heinrich, *J. Appl. Phys.* **44**, 1804 (1973).
- ³⁹H. Mazaki, Y. Ueda, Y. Aihara, T. Kubozoe, and K. Kosuge, *Jpn. J. Appl. Phys.* **28**, L368 (1989).
- ⁴⁰R. B. Goldfarb and J. V. Minervini, *Rev. Sci. Instrum.* **55**, 761 (1984).
- ⁴¹A. J. de Vries and J. W. M. Livius, *Appl. Sci. Res.* **17**, 31 (1967).
- ⁴²H. A. Groenendijk, A. J. van Duyneveldt, and R. D. Willett, *Physica B* **101**, 320 (1980).
- ⁴³L. D. Landau, E. M. Lifshitz, and L. P. Pitaevskii, *Electrodynamics of Continuous Media*, 2nd ed. (Pergamon, Oxford, 1984), p. 273.
- ⁴⁴R. B. Goldfarb and A. F. Clark, *IEEE Trans. Magn.* **MAG-21**, 332 (1985).
- ⁴⁵R. W. Rollins and J. Silcox, *Phys. Rev.* **155**, 404 (1967).
- ⁴⁶F. Gömöry and P. Lobotka, *Solid State Commun.* **66**, 645 (1988).
- ⁴⁷M. Nikolo and R. B. Goldfarb, *Phys. Rev. B* **39**, 6615 (1989).
- ⁴⁸B. Renker, I. Apfelstedt, H. Küpfer, C. Politis, H. Rietschel, W. Schauer, H. Wühl, U. Gottwick, H. Kneissel, U. Rauchsichwalbe, H. Spille, and F. Steglich, *Z. Phys. B* **67**, 1 (1987).
- ⁴⁹H. Mazaki, M. Takano, Y. Ikeda, Y. Bando, R. Kanno, Y. Takeda, and O. Yamamoto, *Jpn. J. Appl. Phys.* **26**, L1749 (1987).
- ⁵⁰D.-X. Chen, R. B. Goldfarb, J. Nogués, and K. V. Rao, *J. Appl. Phys.* **63**, 980 (1988).